4190 *Chem. Mater.* **2006,** *18,* 4190−4194

# Highly Enhanced Luminescence from Single-Crystalline $C_{60}$·1*m*-xylene Nanorods

Lin Wang, Bingbing Liu,* Shidan Yu, Mingguang Yao, Dedi Liu, Yuanyuan Hou,
Tian Cui, and Guangtian Zou

*National Laboratory of Superhard Materials, Jilin University, Changchun 130012, China*

Bertil Sundqvist

*Department of Physics, Umeå University, S-90187 Umeå, Sweden*

Han You, Dingke Zhang, and Dongge Ma

*State Key Laboratory of Polymer Physics and Chemistry, Changchun Institute of Applied Chemistry,
Chinese Academy of Sciences, Changchun 130022, PR China*

*Received April 29, 2006. Revised Manuscript Received June 20, 2006*

Single-crystalline $C_{60}$·1*m*-xylene nanorods with a hexagonal structure were successfully synthesized by evaporating a $C_{60}$ solution in *m*-xylene at room temperature. The ratio of the length to the diameter of the nanorods can be controlled in the range of ≈10 to over 1000 for different applications. The photoluminescence (PL) intensity of the nanorods is about 2 orders of magnitude higher than that for pristine $C_{60}$ crystals in air. Both UV and Raman results indicate that there is no charge transfer between $C_{60}$ and *m*-xylene. It was found that the interaction between $C_{60}$ and *m*-xylene molecules is of the van der Waals type. This interaction reduces the icosahedral symmetry of $C_{60}$ molecule and induces strong PL from the solvate nanorods.

## Introduction

Doped fullerenes have attracted much attention since the doping can alter the charge distributions, the electronic structures, and the energy gaps between the lowest unoccupied molecular orbital (LUMO) and the highest occupied molecular orbital (HOMO) of the parent fullerenes.[1,2] Furthermore, doping might reduce the icosahedral symmetry of $C_{60}$ molecule, making previously forbidden electronic transitions in pristine $C_{60}$ allowed.[3−6] In this way the properties of $C_{60}$ can be tuned by doping various components. As a kind of doped $C_{60}$, $C_{60}$ solvates have also attracted much attention recently from many researchers due to these points.[7−23] Many solvents, including benzene,[12−14] *n*-pentane,[15] hexane,[16] *n*-heptane,[17] $CS_2$,[18,19] and 1,1,2-trichloroethane ($CH_3CCl_3$)[9] have been investigated. It is found that the incorporation of guest molecules into the host $C_{60}$ lattice changes the crystal structure. For example, $C_{60}$ crystals grown in cyclohexane crystallize in the cubic system,[20] $C_{60}$ crystals with $CS_2$[19] or *n*-pentane[15] have orthorhombic structures, and $C_{60}$ solvates grown from benzene[14,21] or *n*-heptane[17] have a hexagonal

---

* Corresponding author. E-mail: liubb@jlu.edu.cn. Tel: +86-431-5168256. Fax: +86-431-5168883.

(1) Hebard, A. F.; Rosseinsky, M. J.; Haddon, R. C.; Murphy, D. W.; Glarum, S. H.; Palstar, T. T.; Ramirez, A. P.; Kotran, A. R. *Nature* **1991**, *350*, 600.

(2) Haddon, R. S.; Hebard, A. F.; Rosseinsky, M. J.; Murphy, D. W.; Duclos, S. J.; Lyons, K. B.; Miller, B.; Rosamilia, J. M.; Fleming, R. M.; Kotran, A. R.; Glarum, S. H.; Makhija, A. V.; Muller, A. J.; Eick, R. H.; Zahurak, S. M.; Tycko, R.; Dabbagh, G.; Thiel, F. A. *Nature* **1991**, *350*, 320.

(3) Wang, Y.; Holden, J. M.; Rao, A. M.; Eklund, P. C.; Venkateswaran, U. D.; Eastwood, DeLyle; Lidberg, R. L.; Dresselhaus, G.; Dresselhaus, M. S. *Phys. Rev. B* **1995**, *51*, 4547.

(4) Wang, Y. *J. Phys. Chem.* **1992**, *96*, 764.

(5) Sassara, A.; Zerza, G.; Chergui, M. *J. Chem. Phys.* **1997**, *107*, 8731.

(6) Zhao, Y.; Fang, Y. *J. Phys. Chem. B* **2004**, *108*, 13586.

(7) Grey, I. E.; Hardie, M. J.; Ness, T. J.; Raston, C. L. *Chem. Commun.* **1999**, 1139.

(8) Talyzin, A.; Jansson, U. *J. Phys. Chem. B* **2000**, *104*, 5064.

(9) Michaud, F.; Barrio, M.; López, D. O.; Tamarit, J. Ll.; Agafonov, V.; Toscani, S.; Szwarc, H.; Céolin, R. *Chem. Mater.* **2000**, *12*, 3595.

(10) Barrio, M.; López, D. O.; Tamarit, J. Ll.; Espeau, P.; Céolin, R.; Allouchi, H. *Chem. Mater.* **2003**, *15*, 288.

(11) Céolin, R.; Tamarit, J. L.; Barrio, M.; López, D. O.; Espeau, P.; Allouchi, H.; Papoular, R. J. *Carbon* **2005**, *43*, 417.

(12) Bürgi, H. B.; Restori, R.; Schwarzenbach, D.; Balch, A. L.; Lee, J. W.; Noll, B. C.; Olmstead, M. M. *Chem. Mater.* **1994**, *6*, 1325.

(13) He, H.; Barras, J.; Foulkes, J.; Klinowski, J. *J. Phys. Chem. B* **1997**, *101*, 117.

(14) Meidine, M. F.; Hitchcock, P. B.; Kroto, H. W.; Taylor, R.; Walton, D. R. M. *J. Chem. Soc., Chem. Commun.* **1992**, 1534.

(15) Pekker, S.; Faigel, G.; Fodor-Csorba, K.; Gránásy, L.; Jakab E.; Tegze, M. *Solid State Commun.* **1992**, *83*, 423.

(16) Toscani, S.; Allouchi, H.; Tamarit, J. L.; López, D. O.; Barrio, M.; Agafonov, V.; Agafonov, V.; Rassat, A.; Szwarc, H.; Céolin, R. *Chem Phys. Lett.* **2000**, *330*, 491.

(17) Ceolin, R.; Agrafonov, V.; Bachet, B.; Gonthiervassal, A.; Szwarc, H.; Toscani, S.; Keller, G.; Fabre, C.; Rassat, A. *Chem. Phys. Lett.* **1995**, *244*, 100.

(18) Shi, X. D.; Kortan, A. R.; Williams, J. M.; Kini, A. M.; Savall, B. M.; Chaikin, P. M. *Phys. Rev. Lett.* **1992**, *68*, 827.

(19) Kikuchi, K.; Suzuki, S.; Saito, K.; Shiromaru, H.; Zakhidov, A. A.; Ugawa, A.; Imaeda, K.; Inokuchi H.; Yakushi, K. *Physica C* **1991**, *415*, 185.

(20) Gorun, S. M.; Creegan, K. M.; Sherwood, R. D.; Cox, D. M.; Day, V. W.; Day, C. S.; Upton, R. M.; Briant, C. E. *J. Chem. Soc., Chem. Commun.* **1991**, 1556.

(21) Balch, A. L.; Lee, J. W.; Noll, B. C.; Olmstead, M. M. *J. Chem. Soc., Chem. Commun.* **1993**, 56.

(22) Graja, A.; Swietlik, R. *Synth. Met.* **1995**, *70*, 1417.

(23) Swietlik, R.; Byszewski, P.; Kowalska, E. *Chem. Phys. Lett.* **1996**, *254*, 73.

10.1021/cm060997q CCC: $33.50

lattice. In addition, it is most interesting that different shapes of solvate crystals form from different solvents. Taking 1,1,2-trichloroethane and bromotrichloromethane ($BrCCl_3$) as examples, the $C_{60}$ 1:1 solvate formed with 1,1,2-trichloroethane[9] shows a needlelike shape with a polyhedral cross section, but $C_{60}$•$2BrCCl_3$[10] shows interpenetrating hexagonal single crystals, thus indicating that the polymorphism of $C_{60}$ is solvent-dependent. Furthermore, the doping with guest molecules can also change the vibrational properties and thus the Raman and IR (infrared absorption) spectra of $C_{60}$. For example, compared to those of pristine $C_{60}$, some of the original peaks shifted and new peaks appeared in the Raman spectra of $C_{60}$ solvates formed in solvents such as benzene and toluene.[8] Graja et al. reported that the guest molecules can also hinder the rotation of $C_{60}$ molecules which leads to a decrease of vibrational−rotational couplings.[22,23] It is therefore very interesting to study the solvent-dependent polymorphism and the properties of $C_{60}$ solvates formed with various solvents.

Another recent development is that one-dimensional nanostructures such as wires, rods, and tubes have become the focus of intensive research owing to their potential applications in electronic, optoelectronic, and electromechanical devices with nanometer scale dimensions as interconnects and/or functional units.[24−27] In addition, the photoluminescence of $C_{60}$ solvates has rarely been studied before. Combining our interests in the potential applications of one-dimensional materials with our interest in the solvent-dependent polymorphism and photoluminescence properties of $C_{60}$ solvates, we have made efforts to synthesize one-dimensional crystals of $C_{60}$ solvates. In this paper we present the synthesis of single-crystalline $C_{60}$•1 *m*-xylene rods on a large scale. All the obtained samples are rod shaped with dimensions in the nanometer range. A photoluminescence (PL) study shows that $C_{60}$•1*m*-xylene nanorods have a strong luminescence which gives potential applications in the optical field.

## Experimental Section

The nanorods of $C_{60}$•1*m*-xylene were synthesized by evaporating a solution of $C_{60}$ in *m*-xylene at room temperature. The nanorods can grow on various substrates such as glass and silicon, which do not react chemically with the solvent and $C_{60}$. After the evaporation, $C_{60}$•1*m*-xylene solvated nanorods with diameters ranging from less than 50 nm to hundreds of nanometers were found on the substrate surface. In contrast to the pure solvent-free $C_{60}$ rod-shaped crystals reported previously,[28] the present as-grown nanorods contain *m*-xylene in the molar ratio $C_{60}$:$C_8H_{10}$ = 1:1. The obtained nanorods were characterized by means of scanning electron microscopy (SEM, SSX-550 Saimadzu, Japan), infrared spectroscopy (IR, Nicolet Avatar 370 DTGS), thermogravimetric analysis (TGA, Perkin-Elmer), X-ray diffraction (XRD, Rigaku D/max-RA), and transmission electron microscopy (TEM, JEM-2010, Japan). The PL and Raman spectra of the nanorods and pristine $C_{60}$ were detected by a Raman spectrometer (Renishaw inVia, U.K.) with either a 514.5 nm or a 830 nm laser as excitation. The ultraviolet−visible (UV) absorption spectra were measured with a UV spectrometer (UV-3150, Saimadzu, Japan) to study the electronic states of the nanorods. All measurements were carried out at room temperature.

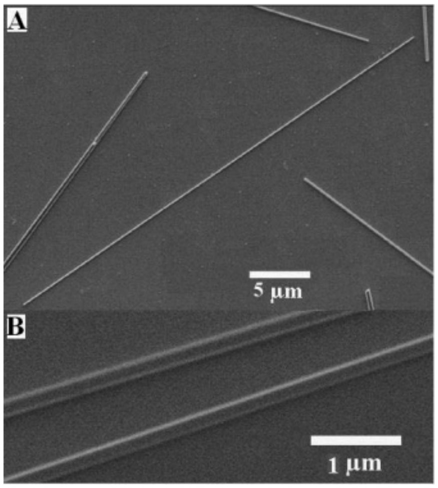

**Figure 1.** SEM images of as grown $C_{60}$•1*m*-xylene nanorods produced by evaporation of a saturated solution of $C_{60}$ in *m*-xylene: (A) many $C_{60}$•1*m*-xylene nanorods grow on a silicon substrate; (B) in large magnification.

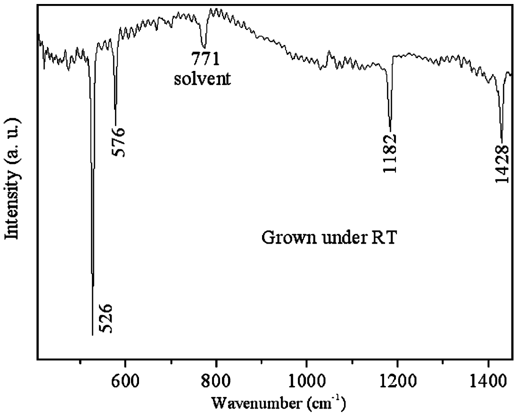

**Figure 2.** IR spectrum of the $C_{60}$•1*m*-xylene nanorods.

## Results and Discussion

A representative morphological study of the nanorods is presented in Figure 1. Figure 1A,B shows SEM images. It is found that the as-grown samples are rod-shaped with diameters in the range of nanometers. The average length is tens of micrometers. It is seen that there is no physical contact between individual nanorods, which is a large benefit for future separation, operation, and applications in the field of nanometer scale devices.

IR spectroscopy has been carried out to study whether the nanorods consist of $C_{60}$ solvate. Figure 2 shows the IR spectrum of the nanorods. There are five obvious absorption peaks in the studied range. The absorption peak at about 770 $cm^{-1}$ is found to belong to the solvent, thus indicating the presence of solvent in the as-grown nanorods. The other four absorption peaks with positions at 526, 576, 1182, and 1428 $cm^{-1}$ are from $C_{60}$. This indicates that the as-grown nanorods are not only made from $C_{60}$ but also contains some solvent, suggesting that they are $C_{60}$ solvates.

---

(24) Hong, S. H.; Zhu, J.; Mirkin, C. A. *Science* **1999**, *286*, 532.
(25) Hu, J.; Odom, T. W.; Lieber, C. M. *Acc. Chem. Res.* **1999**, *32*, 435.
(26) Xia, Y. N.; Yang, P. D.; Sun, Y. G.; Wu, Y. Y.; Mayers, B.; Gates, B.; Yin, Y. D.; Kim, F.; Yan, H. Q. *Adv. Mater.* **2003**, *15*, 353.
(27) Wang, Z. L. *Adv. Mater.* **2000**, *12*, 1295.
(28) Wang, L.; Liu, B. B.; Liu, D. D.; Yao, M. G.; Hou, Y. Y.; Yu, S. D.; Cui, T.; Li, D. M.; Zou, G. T.; Iwasiewicz, A.; Sundqvist, B. *Adv. Mater.* **2006**, *18*, 1883.

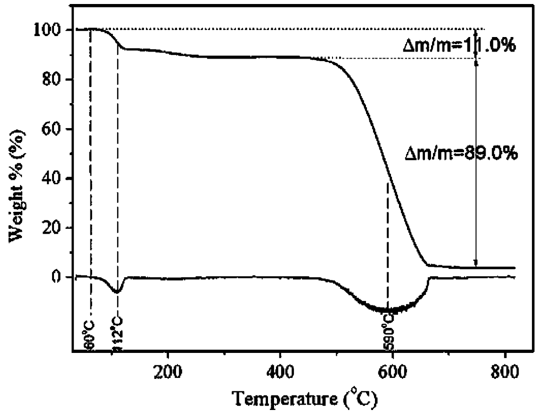

**Figure 3.** TGA curve and its time derivative of the $C_{60}$•1*m*-xylene nanorods.

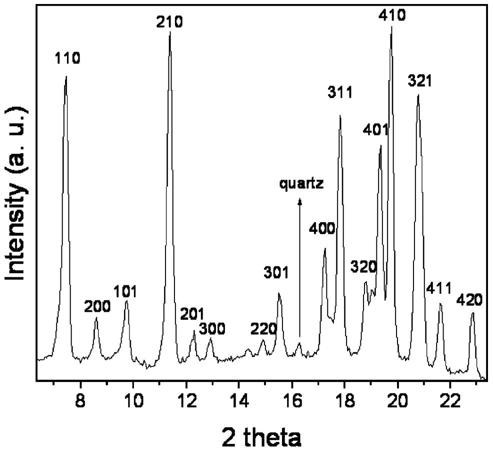

**Figure 4.** XRD pattern of the $C_{60}$•1*m*-xylene nanorods.

Thermogravimetry analysis (TGA), with the temperature ramped from 30 to 800 °C at a rate of 5 °C/min in an Ar atmosphere, was employed to determine the stoichiometry of the $C_{60}$ solvate and to study the thermal behavior of the solvate nanorods. The TGA curve and its time derivative are shown in Figure 3. Clearly, there are two mass loss regions in the studied range of temperature. From a careful analysis of the curves, it is found that the first mass loss starts at about 60 °C. This indicates that the solvate of $C_{60}$ is stable at temperatures lower than 60 °C. This is an advantage for applications at room temperature. Moreover, the mass loss rate has a maximum as the temperature reaches about 112 °C which is close to the boiling temperature of *m*-xylene (135 °C), indicating that this mass loss is due to the evaporation of *m*-xylene. In the high-temperature region the mass loss rate has a second maximum at about 590 °C which is close to the sublimation temperature of $C_{60}$ under ambient pressure. This indicates that the second mass loss comes from the sublimation of $C_{60}$. It is also found that the mass loss of the solvent corresponds to about 11.4% of the total weight which is close to the ideal value (12.8%) for the $C_{60}$:$C_8H_{10}$ = 1:1 molar ratio, suggesting the sample is $C_{60}$•1*m*-xylene.

To confirm the structure of the nanorods, we carried out an X-ray diffraction (XRD) study. The XRD pattern of the as grown nanorods measured at room temperature is shown in Figure 4. This pattern shows that the structure of the nanorods is different from the fcc structure of pure $C_{60}$. The structure has been indexed by a hexagonal system with cell dimensions $a = 2.376$ nm and $c = 1.008$ nm ($a/c = 2.357$), which is similar to that reported by Ramm et al. for bulk crystals obtained by slowly evaporating an *m*-xylene solution of $C_{60}$ ($P6_3$ space group, $a = 2.369(4)$ nm and $c = 1.0046(2)$ nm at 100 K).[29] Their simulations indicate that the solvent molecules are placed at the 3-fold axis and near the $6_3$ screw axis. We further used high-resolution transmission electron microscopy (HRTEM) to study a single nanorod to determine the crystal structure details, such as the growth direction of the nanorods, in detail. A TEM image with a HRTEM image as inset is shown in Figure 5. Again, $C_{60}$ nanorods with dimensions in the nanometer range are observed. The HRTEM image shows that the synthesized $C_{60}$ nanorods are single-crystalline. The lattice spacing of about 1.17 nm between adjacent lattice planes in the image corresponds to the distance between two (110) crystal planes in the structure indexed by the XRD, showing that the axial direction (001) is the preferred growth direction for the as-grown $C_{60}$-solvated nanorods.

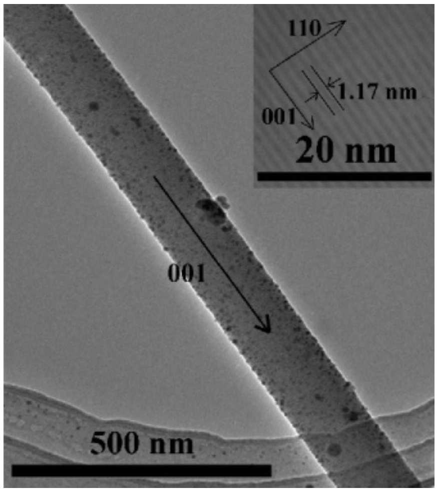

**Figure 5.** TEM image with HRTEM inset of the $C_{60}$•1*m*-xylene nanorods.

We tried to synthesize $C_{60}$ solvate nanorods on various substrates such as glass, silicon, diamond, and metals, including iron, copper, and molybdenum, by evaporating the solution of $C_{60}$ in *m*-xylene at room temperature. Similar nanorods were observed by SEM and TEM to grow on all these substrates, thus indicating that the growth is independent of substrates which is an advantage for potential applications in nanometer scale devices on different substrates.

The PL spectra of the samples were measured under ambient conditions. To avoid the photopolymerization of $C_{60}$, the irradiation power in the focus spot was kept below 1 $\mu$W, which corresponds to an average power density of $\approx$10 mW/mm$^2$. For comparison, pristine $C_{60}$ was studied under the same conditions. The PL spectra of both the nanorods and pristine $C_{60}$ are shown in Figure 6A. The PL spectrum of pristine $C_{60}$ was multiplied by 2 and is in good agreement with previous reports on pristine $C_{60}$.[3,30-32] From the

---

(29) Ramm, M.; Luger, P.; Zobel, D.; Duczek, W.; Boeyens, J. C. A. *Cryst. Res. Technol.* **1996**, *31*, 43.

(30) Rao, A. M.; et al. *Appl. Phys. A* **1997**, *64*, 231.

(31) Zhao, T. N.; Liu J. Q.; Li, Y. L.; Zhu, D. B. *Appl. Phys. Lett.* **1992**, *61*, 1028.

(32) Bashkin, I. O.; et al. *Chem. Phys. Lett.* **1997**, *272*, 32.

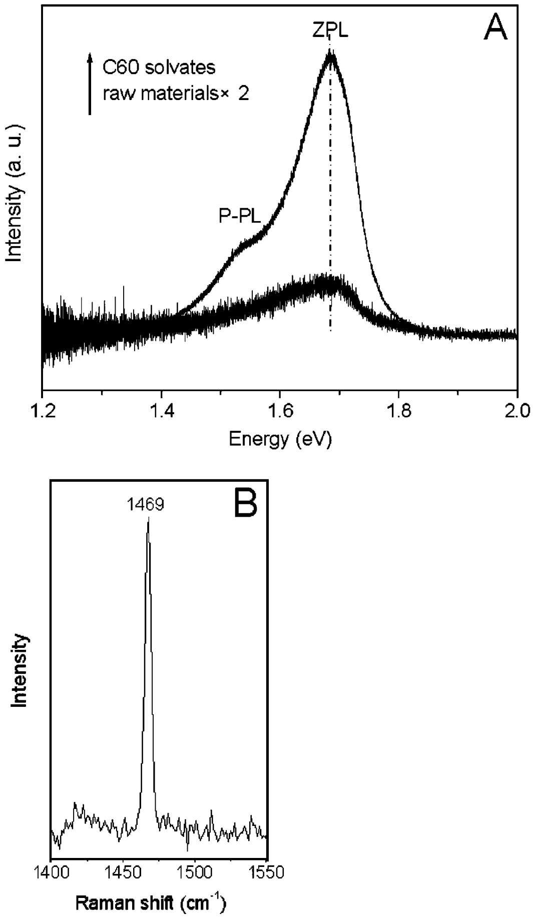

**Figure 6.** (A) PL spectra of the $C_{60}$·1*m*-xylene nanorods and pristine $C_{60}$ powder. Note that the PL spectrum of pristine $C_{60}$ powder is multiplied by 2. (B) Raman spectrum (near the $A_g(2)$ mode) of the same rods, measured at the same spot immediately after the measurements of the PL spectra.

comparison, it is obvious that the PL intensity of the nanorods is about 2 orders of magnitude higher than for pristine $C_{60}$ crystals in air, indicating that the doping by *m*-xylene greatly enhances the luminescence of $C_{60}$. Except for the strong intensity the PL spectrum of the nanorods has features similar to those of pristine $C_{60}$, and there is no shift in the PL spectrum of the solvates compared to pristine $C_{60}$. This suggests that the strong luminescence originates from $C_{60}$ itself. It is seen that the PL spectrum contains two emission bands which are known as the zero-phonon line (ZPL), corresponding to a direct exciton−polaron recombination, and a phonon replica, "P−PL", respectively.[33,34] According to previous works, the ZPL emission band is attributed to an exciton−polaron recombination in $C_{60}$.[33,34] Furthermore, it is well-known that the photopolymerization of $C_{60}$ will change the PL properties of $C_{60}$. So, to test whether photopolymerization occurs during the PL measurements, the Raman spectrum of the rods in the vicinity of the $A_g(2)$ mode was measured at the same spots immediately after the detections of PL spectra. The Raman spectrum (Figure 6B) shows that the $A_g(2)$ mode of the rod is located at 1469 cm$^{-1}$ indicating that the sample is not polymeric $C_{60}$. This suggests that the enhancement of the PL spectra is attributed to the doping by *m*-xylene.

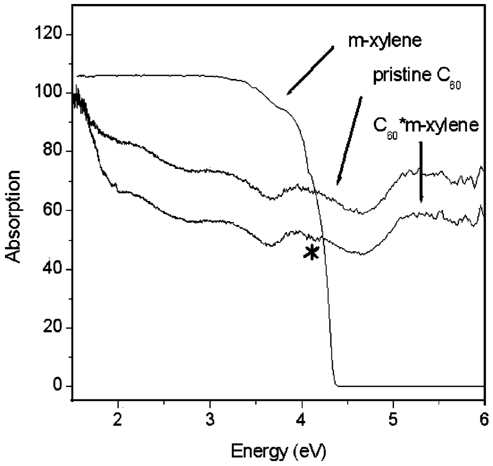

**Figure 7.** UV absorption of the $C_{60}$ solvate rods, pristine $C_{60}$, and *m*-xylene.

The UV absorption spectrum has been measured by using an integrating sphere to study the electronic states of the solvate. For comparison, pristine $C_{60}$ and *m*-xylene have also been studied under the same conditions. The UV spectra of the solvates, pristine $C_{60}$, and *m*-xylene are shown in Figure 7. The UV absorption spectrum we obtained for pristine $C_{60}$ is consistent with that of previous reports.[3,35] In a comparison with the absorption spectrum of pristine $C_{60}$, a new absorption band at about 4.1 eV (asterisk) is present in the UV absorption spectrum. This position is close to the absorption edge of *m*-xylene, suggesting the absorption is the contribution from *m*-xylene. Once more, the obtained nanorods prove to be solvated $C_{60}$. In addition, there is no obvious shift of the absorption bands between pristine and solvated $C_{60}$, indicating that the effect of doping by *m*-xylene on the electronic state of the $C_{60}$ molecules is too small to detect with UV spectroscopy. A comparison of the two UV spectra shows that the absorption coefficient of the $C_{60}$ solvate is larger than that of pristine $C_{60}$, indicating a higher quantum yield for $C_{60}$ solvate. We also measured the quantum yield of the as-grown nanorods by using an integrating sphere. The quantum yield of the nanorods is $2.0 \times 10^{-3}$, which is about 1−2 orders of magnitude higher than reported earlier for $C_{60}$.[4,36,37]

It is known that the fluorescence quantum yield of $C_{60}$ is very low due to symmetry restrictions.[3−6] However, environmental effects, for example, the doping effect, could relax the selection rules by reducing the symmetry of $C_{60}$ and lead to a high fluorescence radiation rate. For the purpose to make clear how the *m*-xylene molecules enhance the PL of the solvates, Raman spectroscopy with a 830 nm wavelength laser as excitation was employed to study the lattice vibrations of a solvate grown on silicon substrate. The Raman spectrum is shown in Figure 8. The peak located at 520 cm$^{-1}$ is the contribution from silicon, showing that the obtained spectrum is reliable. The 10 Raman active modes of $C_{60}$ have

---

(33) Leach, S.; Vervloet, M.; Deprès, A.; BreH heret, E.; Hare, J. P.; Dennis, T. J.; Kroto, H. W.; Taylor, R.; Walton, D. R. M. *Chem. Phys.* **1992**, *160*, 451.

(34) Capozzi, V.; Trovato, T.; Berger, H.; Lorusso, G. F. *Carbon* **1997**, *35*, 763.

(35) Kazaoui, S.; Ross, R.; Minami, N. *Solid State Commun.* **1994**, *90*, 623.

(36) Sun, Y. P.; Wang, P.; Hamilton, N. B. *J. Am. Chem. Soc.* **1993**, *115*, 6378.

(37) Catalh J.; Elguerot, J. *J. Am. Chem. Soc.* **1993**, *115*, 9249.

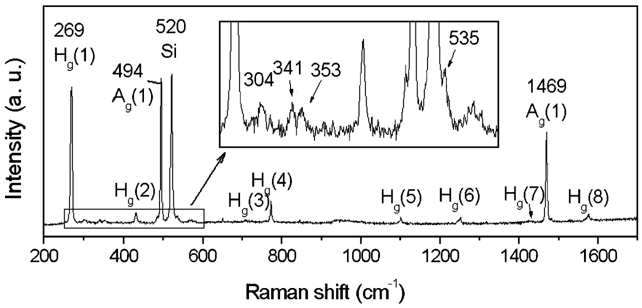

**Figure 8.** Raman spectrum of the $C_{60}$ solvate rods.

been pointed out. Obviously, the $A_g(2)$ mode, one of the modes most sensitive to charge transfer in $C_{60}$, is located at 1469 $cm^{-1}$, the same position as in pristine $C_{60}$, indicating the absence of charge transfer in the compound. In addition, it is also found that there are some unknown peaks with positions at 304, 341, 353, and 535 $cm^{-1}$ present. Furthermore, in comparison with the spectrum of pure $C_{60}$, the $H_g(1)$ (272 $cm^{-1}$) and $A_g(1)$ (496 $cm^{-1}$) modes in this spectrum shift to 269 and 494 $cm^{-1}$, respectively. Similar shifts and new peaks have also been found in the Raman spectra of $C_{60}$ solvates formed with toluene and hexane.[8] They were attributed to the presence of the guest molecules, lattice disorder, and weak van der Waals interactions between the $C_{60}$ molecules and the solvents, which all reduce the symmetry of the $C_{60}$ lattice.

It is clear now that a van der Waals interaction is present between $C_{60}$ and *m*-xylene molecules in the $C_{60}$ solvate nanorods and that this reduces the icosahedral symmetry of the $C_{60}$ molecule. The electric-dipole transitions which were forbidden in pristine $C_{60}$ due to the high symmetry are allowed in this lower symmetry. As a result the quantum yield and PL intensity are enhanced greatly.

## Conclusion

In summary we successfully synthesized single-crystalline $C_{60}$•1*m*-xylene nanorods with a hexagonal structure. The ratio of the length to the diameter of the nanorods can be controlled in the range of ≈10 to over 1000 for different applications. Both UV and Raman results indicate that there is no charge transfer between $C_{60}$ and *m*-xylene. The interaction between $C_{60}$ and *m*-xylene molecules is of the van der Waals type. This interaction reduces the icosahedral symmetry of $C_{60}$ molecule and induces strong PL from the solvate nanorods. The PL intensity of the nanorods is about 2 orders of magnitude higher than that for pristine $C_{60}$ crystals in air.

**Acknowledgment.** This work was supported financially by the NSFC (Grant Nos. 10144004, 10204010, and 10574053), the RFDP (Grant No. 20020183050), the Trans-Century Training Program Foundation for the Talents, the Cultivation Fund of the Key Scientific and Technical Innovation Project (Grant No. 2004-295) of MOE of China, the National Basic Research Programm of China (Grant No. 2005CB724400), the Project for Scientific and Technical Development of Jilin province, and also by an exchange grant from the Swedish Research Council through the SIDA-Swedish Research Links exchange program.

CM060997Q